SOME PROBLEMS IN OPTICAL OCEANOGRAPHY[1]

By

CHARLES COX AND WALTER MUNK

Scripps Institution of Oceanography

ABSTRACT

Problems involving the refraction and reflection of light from sun and sky by a *roughened* sea surface have been made accessible to numerical treatment by measurements of the probability distribution of sea surface slopes. Four cases are treated. (1) The refracted sun's glitter, as seen from beneath the surface. It is smaller but about 1000 times more luminous (neglecting absorption) than the reflected glitter, and, unlike the reflected glitter, it expands and dims as the sun sets. (2) The albedo of a rough surface to direct sunlight. It is slightly larger at high sun angles and substantially smaller at low sun angles than the albedo of a flat surface. Accordingly, more solar energy penetrates arctic waters than had been estimated previously and the amount of this additional energy depends upon wind speed. (3) The luminosity and albedo of a rough sea surface due to sky light. At the horizon a rough surface is darker than a smooth surface, thus enhancing the horizon contrast. The albedo of the sea surface to sky light varies from 5 to 10%, depending on the distribution of illumination from the sky; it is largest when the sea is flat calm. The roughening by a Beaufort 4 wind reduces the albedo by about 20%. (4) The visibility of slicks.

1. INTRODUCTION

Measurements of the probability distribution of slopes have been made by Duntley (1950), Schooley (1954), and by Cox and Munk (1954a and b). As a result of these measurements, certain oceanographic problems have become accessible to numerical treatment. In these problems we are concerned with the *average* brightness ("radiance" in optical terminology) of the sea surface due to sun or sky when viewed from above or beneath. The average is formed over sufficient time or sufficient surface area to smooth out fluctuations such as the ones that result from individual glitter sparkles of sunlight. The average is then essentially independent of time but varies smoothly with the azimuth and elevation of the portion of sea surface under consideration.

[1] Contribution from the Scripps Institution of Oceanography, New Series No. 776. This work has been sponsored in part by the Geophysics Research Directorate of the Air Force Cambridge Research Center, Air Research and Development Command, under Contract No. AF(19) 604 (1053).

Let $z(x, y)$ designate the elevation of the sea surface above a mean level and let $\partial z/\partial x = z_x$, $\partial z/\partial y = z_y$ be the corresponding slope components. We shall require the probability $p(z_x, z_y)\delta z_x \delta z_y$ that the slope components will lie within the limits $z_x \pm \frac{1}{2}\delta z_x$, $z_y \pm \frac{1}{2}\delta z_y$. As a first approximation, we find (Cox and Munk, 1954a: section 6.3) that the distribution is Gaussian,

$$p(z_x, z_y) = (\pi\sigma^2)^{-1} \exp\left[-(z_x^2 + z_y^2)/\sigma^2\right] . \tag{1}$$

The mean square slope, regardless of direction, $\sigma^2 = < z_x^2 + z_y^2 >_{AV}$, increases with the "masthead" wind speed in $m\ s^{-1}$, W, according to

$$\sigma^2 = .003 + 5.12 \times 10^{-3} W \pm .004 . \tag{2}$$

In the presence of a slick this value is reduced by a factor of two or three.

In adopting the isotropic Gaussian distribution function (1) we simplify our results at the cost of omitting certain observed effects of wind directionality. For it has been found (Cox and Munk, 1954a: sections 6.3, 6.4) that the up/downwind slope components exceed the crosswind components and that the up/downwind distribution is skewed.

2. THE GLITTER AS SEEN FROM BENEATH THE SURFACE

The same glitter pattern differs substantially when viewed from above and below the sea surface. These differences are illustrated in Fig. 1 and are described in the legend. The upper part of Fig. 1 is based on the theory of *reflected* glitter as given previously (Cox and Munk, 1954a: sections 3.1, 3.2). The theory for *refracted* glitter (lower part of Fig. 1) is developed along similar lines in the following sections.

The principal differences between the reflected and refracted glitter patterns are as follows: (1) The reflected glitter pattern is larger[2] and less luminous than the refracted pattern. (2) The reflected pattern shrinks and becomes more luminous as the sun sets; the reverse holds for the refracted pattern. (3) Both reflected and refracted patterns move toward the horizon with the setting sun, but the reflected pattern moves almost twice as fast.

In a general way these conclusions are in agreement with what has been observed. However, at ordinary diving depths the luminescence varies considerably with the passage of individual waves, whereas the patterns described here correspond to suitable time exposures. The fluctuations diminish with increasing depth, so that at a depth of, say

[2] The refracted patterns in Fig. 1 are enlarged by a factor of 2.5 relative to the reflected patterns.

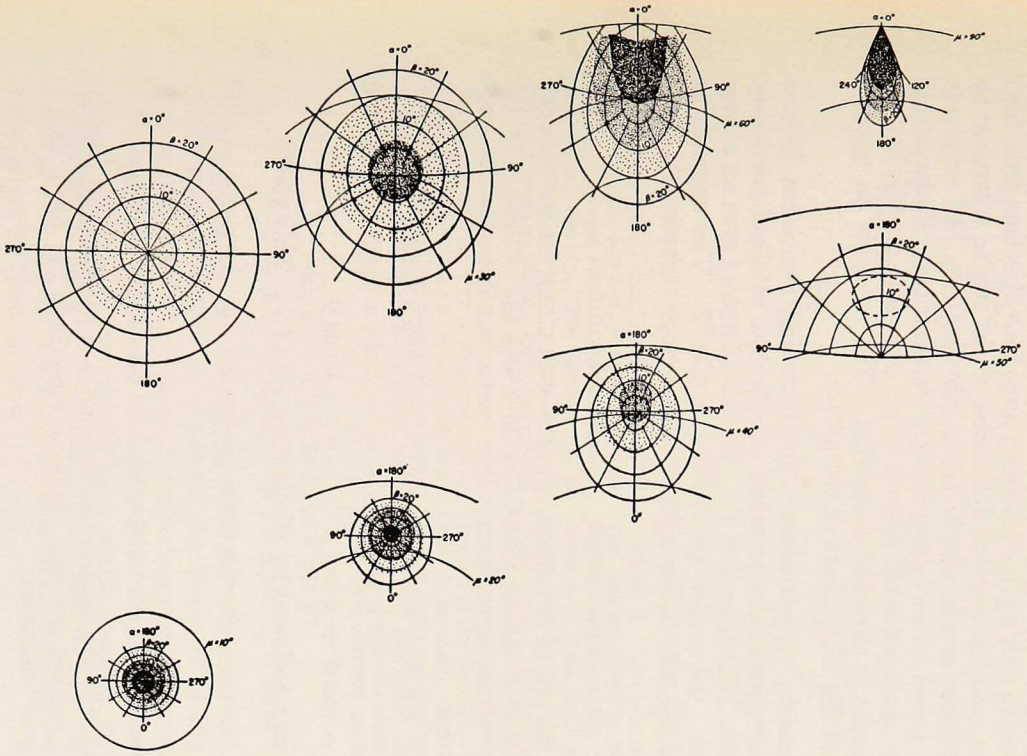

Figure 1. The glitter patterns for a Beaufort 4 wind ($W = 7\ ms^{-1}$, $\sigma = 0.2$) as seen from above the surface (UPPER FOUR) and from beneath (LOWER FOUR). The patterns from left to right are drawn for solar zenith angles of 0° (sun at zenith), 30°, 60°, 90° (sun at horizon). Each pattern is drawn with reference to the polar coordinates μ, the observer's zenith angle, and ν, the azimuth relative to the sun (see Fig. 2). The value $\mu = 0°$ designates a point on the surface directly beneath (above) the observer; the horizon is at $\mu = 90°$. The circular arcs in the upper patterns are drawn for $\mu = 30°, 60°, 90°$, in the lower patterns for 10°, 20°, . . . 60°, 70°. The μ-scale in the lower figure is 2.5 times the scale in the upper figures. For each diagram the radial α-lines give the azimuth of ascent, and the quasi-elliptical β-lines the tilt required for the occurrence of a highlight (Fig. 2). Shadings indicate surface luminosity. The values in units of the sun's luminosity are as follows:

shading	*none*	*light*	*medium*	*heavy*
upper figures: (parts per million)	$<.66$	.66–3.3	3.3–16.6	>16.6
lower figures: (parts per thousand)	$<.25$	.25–1.3	1.3– 6.6	>6.6

1000 feet, the observed pattern would resemble the computed pattern rather closely were it not for the effect of absorption (which we have ignored) and other difficulties.

Whitecaps have been neglected. At low sun angles the effects of multiple scattering and wave shadowing introduce a serious error into our calculation, and the angular dimension of the sun as compared to the reflected pattern should also be taken into account. All constants have been computed for an isotropic slope distribution. Under actual conditions, the most probable slope is a few degrees, not zero, and its azimuth of ascent is directed downwind. The result is an upwind displacement of the bright core of the glitter.

2.1. *The geometry of refraction.* The following derivation follows closely the derivation of the geometry of reflection attained previously (Cox and Munk, 1954a: section 3). We can therefore give an abbreviated account. All angles are defined in Fig. 2. The azimuth of ascent, α, and the tilt, β, are related to the slope components z_x, z_y according to

$$z_x = \sin\alpha \tan\beta, \quad z_y = \cos\alpha \tan\beta \,. \tag{3}$$

According to the law of refraction, a unit vector along the incident ray *minus* a vector of length n along the refracted ray[3] equals a vector normal to the refracting surface. This vector equation has the components

$$\begin{aligned} -\sin\psi - n\sin\mu\cos\nu &= -k\cos\alpha\sin\beta \\ -n\sin\mu\sin\nu &= -k\sin\alpha\cos\beta \\ -\cos\psi + n\cos\mu &= k\cos\beta \,. \end{aligned} \tag{4}$$

The factor k may be found by eliminating μ and ν. This yields

$$k = n\cos\omega_r - \cos\omega \tag{5}$$

where

$$\cos\omega = \cos\beta\cos\psi - \cos\alpha\sin\beta\sin\psi, \quad n^{-1}\sin\omega_r \sin\omega \,.$$

It can be verified that ω and ω_r are the angles of incidence and refraction with the surface normal. Solving equations (4) for μ and ν, we find the "grid" relations:

[3] The index of refraction, n, depends on the frequency of light. In the subsequent calculations we have assumed a value $n = 1.34$ corresponding to yellow light. This value is an appropriate average for phenomena depending on the total energy of sunlight.

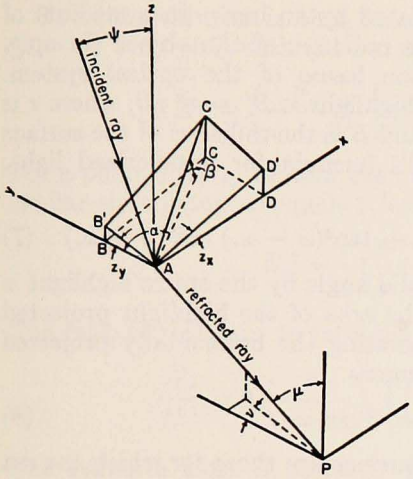

Figure 2. The coordinate system is centered at the sea surface with the z-axis vertically upward and the y-axis horizontal and toward the sun. The incident ray is refracted at A toward the observer at P, where it forms an angle μ with the vertical, and an azimuth ν to the right of the sun. Points ABCD define a horizontal plane through A, and $AB'C'D'$ a plane tangent to the sea surface. The tilt, β, is measured in the direction, AC, of steepest ascent, and this direction makes an angle α to the right of the sun.

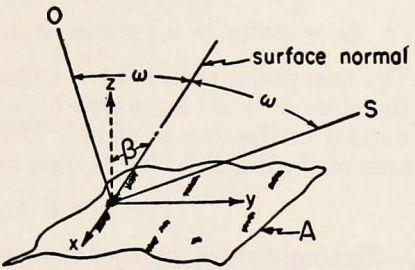

Figure 3. "A" is a unit of sea surface. The shaded portions indicate all points where the slopes lie within designated limits $z_x \pm \frac{1}{2}\delta z_x$, $z_y \pm \frac{1}{2}\delta z_y$. The average tilt in the shaded areas is β, where $\tan^2\beta = z_x^2 + z_y^2$. The y-axis is drawn away from the sun. Incident rays from the sun at O are reflected toward S. In the discussion of sky light (Sec. 4), the direction of rays is reversed. Incident rays from the sky at S are reflected toward the observer at O. In *both* cases the angle of the incident ray with the z-axis is designated by ψ and of the reflected ray by μ.

$$\begin{aligned} \cos\mu &= n^{-1}(\cos\psi + k\cos\beta) \\ \cot\nu &= \cot\alpha - (k\sin\alpha\sin\beta)^{-1}\sin\psi\,. \end{aligned} \tag{6}$$

Any point on the sea surface can be characterized by its zenith angle μ and direction ν. In the eight diagrams of Fig. 1, the angles μ, ν are represented by polar coordinates; μ is the radial distance and ν the angular coordinate. On these polar diagrams, curves of constant $\alpha(\mu, \nu)$ and $\beta(\mu, \nu)$ for various solar zenith angles ψ have been drawn according to the grid relations. An observer looking upward to a point μ, ν at the surface will see such facets highlighted that have the slope given by these curves.

2.2. *Surface radiance.* This section corresponds to the previously discussed case of reflection (Cox and Munk, 1954a: section 4). Individual highlights form distorted images of the sun. According to a general law of optics, the radiance (power per unit solid angle per

unit area normal to the beam) radiated by an image in a medium of refractive index n is (n^2) times the radiance of the object (in open space) reduced by any transmission losses of the optical system. Accordingly, the radiance within a highlight is $B' = n^2 \tau B$, where τ is the transmission of the sea surface and B is the radiance of the surface of the sun. According to Fresnel's formula for unpolarized light, $\tau = 1 - \rho$, where

$$2\rho = \sin^2(\omega - \omega_r) \csc^2(\omega + \omega_r) + \tan^2(\omega - \omega_r) \cot^2(\omega + \omega_r) . \quad (7)$$

The *total* power radiated per unit solid angle by the entire highlight is therefore $I = B' \Delta_s$, where Δ_s is the area of the highlight projected normal to the line of sight. Designating the horizontally projected area of the highlight by Δ_h, this becomes

$$I = n^2 \tau B \Delta_h \sec \beta \cos \omega_r . \quad (8)$$

The highlighted areas of the sea surface are those for which the sea surface has the appropriate tilt and azimuth of ascent to satisfy equations (6) within a small "tolerance" which allows for the fact that rays may originate at any point on the sun's face. This imposes limits on the permitted variation of α, β, or alternatively z_x, z_y, within the highlight. It may be shown that the area on the z_x, z_y-plane corresponding to the permitted variation of slopes within a highlight is

$$\delta z_x \, \delta z_y = \epsilon \, k^{-2} \cos \omega \sec^3 \beta , \quad (9)$$

where ϵ is the solid angle subtended by the sun.[4]

The fraction of the (horizontally projected) sea surface which has slope components within the required limits $z_x \pm \frac{1}{2}\delta z_x$, $z_y \pm \frac{1}{2}\delta z_y$, is $p(z_x, z_y)\delta z_x \delta z_y$, where p is the probability distribution of slopes (Eq. 1). Hence the average power radiated by all highlights within a horizontal unit area of sea surface is $p\delta z_x \delta z_y I$. The average radiance N of the sea surface in the line of sight (power per unit solid angle per unit area *normal* to the beam) is this value multiplied by sec μ. Substituting from (8) and (9), we obtain

$$N = n^2 \tau H k^{-2} p \sec^4 \beta \cos \omega_r \cos \omega \sec \mu . \quad (10)$$

Here we have replaced $B\epsilon$ by H, the irradiance (power per unit area) received at the sea surface from the sun.

[4] The solid angle subtended by a highlight is assumed small compared to the angle subtended by the sun. The highlighted areas are of the order of 0.1 mm², so that this assumption holds except within a few centimeters of the sea surface. In addition, the angular size of the sun is assumed to be small compared to the angular dimensions of the glitter pattern. This assumption fails for low sun angles and for very small slopes.

The simplest case is that for a point directly above the observer ($\mu = z_x = z_y = 0$) with the sun at the zenith ($\psi = 0°$). This gives

$$N_0 = \left(\frac{n}{n-1}\right)^2 \left[1 - \left(\frac{n-1}{n+1}\right)^2\right] Hp\,(0,0).$$

For a point directly *beneath* the observer, the reflected radiance under similar circumstances equals (Cox and Munk, 1954a)

$$N_0' = \frac{1}{4}\left(\frac{n-1}{n+1}\right)^2 Hp\,(0,0).$$

The ratio of refracted to reflected radiance is

$$\frac{N_0}{N_0'} = 4\left(\frac{n}{n-1}\right)^2 \left[\left(\frac{n+1}{n-1}\right)^2 - 1\right] \doteq 3000.$$

The radiance from a perfectly diffusing surface (one that scatters uniformly into a solid angle 2π) is H/π.

3. REFLECTION OF DIRECT SUNLIGHT FROM A ROUGH SEA SURFACE

The reflection of direct sunlight is an important factor in the energy budget of the ocean. Estimates based on reflection from a flat water surface are in error because the average coefficient of reflection for a rough surface differs from that for a flat surface. The difference becomes appreciable for low solar elevations.

First we consider the reflection by facets whose slopes lie within the limits $z_x \pm \frac{1}{2}\delta z_x$, $z_y \pm \frac{1}{2}\delta z_y$. Their (horizontally projected) area within a unit area A (Fig. 3) is, on the average, $p(z_x, z_y)\delta z_x \delta z_x$. The actual (tilted) area is sec $\beta p \delta z_x \delta z_y$. The projected area normal to the incoming rays from the sun is cos ω sec β $p\delta z_x \delta z_y$. The radiant flux intercepted is H cos ω sec β $p\delta z_x \delta z_y$. The reflected flux is

$$H\rho(\omega) \cos \omega \sec \beta \; p\delta z_x \delta z_y\,, \tag{11}$$

where $\rho(\omega)$ is given by Fresnel's formula (7). It is assumed that the incident light is not polarized and is reflected only once.

Equation (11) gives the reflected flux associated with slopes within the limit $z_x \pm \frac{1}{2}\delta z_x$, $z_y \pm \frac{1}{2}\delta z_y$. The total reflected flux per unit area of sea surface is then

$$H \iint \rho(\omega) \cos \omega \sec \beta \; p dz_x dz_y\,, \tag{12}$$

with the integration extending over all slopes exposed to the sun.

The radiant flux incident upon the unit area is $H \cos \psi$, where ψ is the sun's zenith angle. Consequently the fraction reflected, i. e. the *albedo*, is

$$R = \sec \psi \iint \rho(\omega) \cos \omega \sec \beta \, p dz_x dz_y . \tag{13}$$

For the special case of a level surface, $z_x = z_y = \beta = 0, \omega = \psi, \rho(z_x, z_y) = 0$ except at $z_x = 0, z_y = 0$. It follows that $R = \rho(\psi)$. For the general case, we make use of the law of reflection (Fig. 3)

$$\cos \omega = \cos \beta(\cos \psi + z_y \sin \psi) . \tag{14}$$

The quantities $F(\omega) = \rho(\omega) \cos \omega$ and $\sec \beta = (1 + z_x^2 + z_y^2)^{\frac{1}{2}}$ may now be expanded in Taylor's series in z_x, z_y around the values $z_x = z_y = 0$ for which $\beta = 0, \omega = \psi$. This yields

$$\mathrm{R} = \rho(\psi) \iint (1 + az_y + bz_y^2 + cz_x^2 + \ldots) \, p dz_x dz_y , \tag{15}$$

where

$$a = -F'/F, \quad b = \tfrac{1}{2} + \tfrac{1}{2}F''/F, \quad c = \tfrac{1}{2} + \tfrac{1}{2}(F'/F) \cot \psi . \tag{16}$$

The functions F, $F' = dF/d\omega$, $F'' = d^2F/d\omega^2$ are evaluated at $\omega = \psi$.

If all slopes are less in magnitude than $90° - \psi$, then the sea surface is everywhere exposed to the sun and the limits are $\pm \infty$. In this case

$$R = \rho(\psi) \, (1 + b < z_y^2 >_{AV} + c < z_x^2 >_{AV}) . \tag{17}$$

Here we have made use of

$$< z_y >_{AV} = \int_{-\infty}^{\infty}\int z_y p dz_x dz_y = 0$$

because the mean sea level is horizontal. To the present approximation the albedo depends only on the components of mean square slope along the sun's azimuth and normal to it; it does not depend on the form of $p(z_x, z_y)$. For the isotropic case, $< z_x^2 >_{AV} = < z_y^2 >_{AV} = \tfrac{1}{2} \sigma^2$, and

$$R = \rho(\psi) \, [1 + f(\psi) \, \sigma^2] , \tag{17a}$$

where

$$f(\psi) = \tfrac{1}{2}(b + c) = \tfrac{1}{2} + \tfrac{1}{4}(F'/F) \cot \psi + \tfrac{1}{4} F''/F \tag{17b}$$

is the "roughness" function plotted in Fig. 4. Some difficulties arise when ψ is large, and these will now be considered.

Large negative slopes in the component z_y are shadowed if they exceed $\cot \psi$. We shall allow for this "first order" hiding by setting the limits $(-\cot \psi)$ to ∞ for z_y (but $\pm \infty$ for z_x). This is equivalent to the limits 0 to 90° in the angle of incidence, ω. Because some additional slopes are hidden, the computed value of R will be too large for large ψ, but the evaluation of the "second order" hiding involves infor-

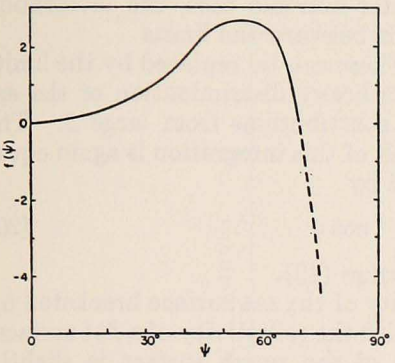

Figure 4. The roughness function $f(\psi)$ as defined in equation (17b). In the dashed portion near the horizon the function is not strictly applicable because of shadowing and multiple reflection.

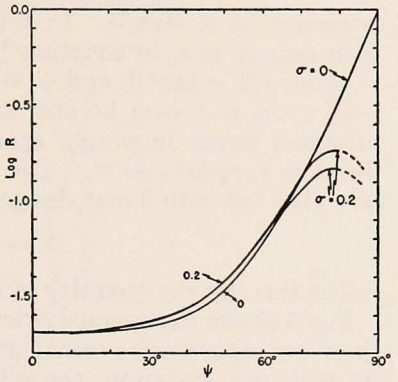

Figure 5. Reflection of solar radiation from a flat surface ($\sigma = 0°$) and a surface roughened by a Beaufort 4 wind ($\sigma = 0.2$). The albedo R varies from .02 for a zenith sun ($\psi = 0°$) to unity for the sun at the horizon ($\psi = 90°$) with the surface flat. For a rough surface, shadowing and multiple reflections become important factors when the sun is low. The lower and upper branches of the curve marked $\sigma = 0.2$ represent two assumptions regarding the effects of multiple reflection. True values are expected to lie between the indicated limits.

mation on the spectrum of ocean waves, and in the absence of such information we must restrict ourselves to the first order hiding.

The integration now yields

$$R = \rho(\psi)\ \{\tfrac{1}{2}[1 + I(k)] + \tfrac{1}{2}\pi^{-\frac{1}{2}} a\sigma e^{-k^2} + \\ + \tfrac{1}{4} b\sigma^2[1 + I(k) - 2\pi^{-\frac{1}{2}} k e^{-k^2}] + \tfrac{1}{4} c\sigma^2[1 + I(k)] + \ldots\} \quad (18)$$

where

$$k = \sigma^{-1} \cot\psi \quad (19)$$

and where $I(k) = 2\pi^{-\frac{1}{2}} \int_0^k e^{-t^2} dt$ is the error integral. The present approximation is adequate for large values of the dimensionless parameter k. For *very* large values, equation (18) converges on (17).

So far we have neglected multiple reflections. If the reflected ray goes toward a point *beneath* the horizon, then certainly there must be at least one further reflection. This "first order" multiple reflection requires that z_y be negative and exceed $\frac{1}{2} \cot\psi(1 - \tan^2\beta)$ in magnitude. The product of coefficients of reflection of all but the first reflection is unknown but must lie between unity and zero. In the first extreme, multiple reflections would not alter R, and equation (18)

is correct as it stands. In the latter extreme case, the integration with respect to z_y in equation (15) is between the limits $-\frac{1}{2}\cot\psi(1-\tan^2\beta)$ and $+\infty$. These can be replaced by the limits $-\frac{1}{2}\cot\psi$ and $+\infty$ because of the heavy discrimination of the exponential factor in $p(z_x z_y)$ against contributions from large β. The limits on z_x remain $\pm\infty$. The result of this integration is again equation (18) but with k now designated by

$$k = \tfrac{1}{2}\sigma^{-1}\cot\psi \tag{20}$$

rather than by the quantity in equation (19).

Fig. 5 shows the average reflectivity of the sea surface bracketed by these two expressions as compared with the reflectivity of a flat surface. At high sun elevation, the albedo of the rough surface is slightly larger; for $\psi = 40°$ the values are 2.5% for the smooth surface and 2.7% for the rough surface. At low sun elevation, increasing roughness leads to a marked decrease in albedo. The only conclusion of oceanographic consequence seems to be that in summer substantially more energy must penetrate the open stretches of the Arctic Ocean than had been estimated previously and that the amount of this additional energy depends on the wind speed.

4. REFLECTION OF SKY LIGHT FROM A ROUGH SURFACE

The radiance of the sky is due to scattering of sunlight and reflected "earth light" by air molecules (Rayleigh scattering), dust, haze, clouds, etc. This varies in a complicated and rather unpredictable way over the sky dome. We shall consider the three cases illustrated in Fig. 6:

(a) a clear tropical sky at Bocaiuva, Brazil, from measurements[5] by Richardson and Hulbert (1949);

(b) a uniform sky dome;

(c) a completely overcast sky, whose radiance can be approximated by the empirical formula (Moon and Spencer, 1942)

$$N_s(\psi) = \tfrac{1}{3}N_s(0)(1 + 2\cos\psi)\,. \tag{21}$$

To simplify subsequent calculations we shall make all quantities depend only on the zenith angle ψ. This already holds for (*b*) and (*c*), but for (*a*) the sky depends largely on zenith angle. Accordingly we have ignored the increased radiance near the sun and have based our calculations on the observed radiance along an azimuth 90° from the azimuth of the sun. In the following calculations we also assume

[5] The observations were made at 2200 feet; the sky radiance at sea level would be slightly different.

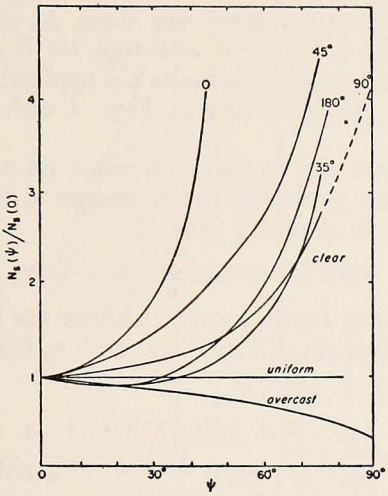

Figure 6. The radiance of the sky $N_s(\psi)$ divided by the radiance at the zenith $N_s(0°)$ as function of the zenith angle ψ. The curves for the clear sky are based on observation at Bocaiuva, Brazil, for the sun at $\psi = 60°$. They are drawn for indicated azimuths relative to the sun. Computations are based on the heavy curve marked 90°. The radiance for the overcast sky, based on the empirical law (21), applies to all azimuths.

unpolarized sky light.[6] Actually there is considerable polarization for a clear sky, and the polarization is a function of the azimuth relative to the sun.

The derivation is similar to that in the preceding section. The rays in Fig. 3 are reversed, with ψ and μ again designating the zenith angles of the incident and reflected rays. The radiant flux from a segment of sky S reflected by the unit area A toward the observer O is (in place of eq. 11)

$$N_s\, \rho(\omega)\, \cos\omega\, \sec\beta\, p\delta z_x \delta z_y\,,$$

where N_s is the radiance of the sky (power per unit solid angle per unit area normal to the beam). Summing over all *visible* slopes yields the total reflected flux from the unit area A toward the observer O,

$$\int\int N_s\, \rho(\omega)\, \cos\omega\, \sec\beta\, p dz_x dz_y\,. \qquad (22)$$

The radiance of the sea surface in the observer's line of sight (intensity per unit area normal to the beam) is found by dividing by $\cos\mu$:

$$N = \sec\mu \int\int N_s\, \rho(\omega)\, \cos\omega\, \sec\beta\, p dz_x dz_y\,. \qquad (23)$$

[6] Effectively we write $[N_{s\parallel} + N_{s\perp}]\,[\rho_\parallel + \rho_\perp]$ (or $N_s\,\rho$ in our notation) instead of $N_{s\parallel}\rho_\parallel + N_{s\perp}\rho_\perp$, where $\parallel$ $\perp$ refer to polarization in the plane of incidence, and normal to it, respectively.

For the special case of a uniform sky dome, N_s is constant, and the expression for (N/N_s) is identical with that for R in section 3. The preceding remarks on integration limits are applicable, and the results given in equations (15)–(20) and in Figs. 4 and 5 can be applied directly.

For the case where sky radiance depends on the zenith angle ψ (and ψ only), we must generalize the procedure in section 3. Writing the law of reflection in the form (Fig. 3)

$$\cos\psi = \cos^2\beta\,[(1 - \tan^2\beta)\cos\mu + 2z_v \sin\mu], \tag{24}$$

and again expanding in Taylor's series, leads to the integrals in section 3 with R now denoting $N(\mu)/N_s(\psi)$, and with a, b, c replaced by

$$\begin{aligned} a_s &= -F'/F - 2N_s'/N_s\,, \\ b_s &= \tfrac{1}{2} + \tfrac{1}{2}F''/F + 2(N_s'/N_s)(F'/F) + 2N_s''/N_s\,, \\ c_s &= \tfrac{1}{2} + \tfrac{1}{2}(F'/F)\cot\mu + 2(N_s'/N_s)\cot\mu\,. \end{aligned} \tag{25}$$

Fig. 7 shows the results for two sky conditions illustrated in Fig. 6. Directly beneath the observer ($\mu = 0°$), the rough sea may be brighter or dimmer than a smooth sea depending on the condition of the sky. A rough sea contrasts with a flat surface most markedly near the horizon, where the rough sea appears darker. If the sea were absolutely flat, then the radiance of the sea surface just beneath the horizon would equal the radiance of the sky just above it, and there would be no visible horizon.

The albedo of the sea surface exposed to sky light is the ratio of reflected to incident flux. The reflected flux from a unit area is $N(\mu)\cos\mu$ (compare equations 22 and 23) and the total reflected flux is $2\pi\int_0^{\frac{1}{2}\pi} N(\mu)\cos\mu\sin\mu\,d\mu$. Similarly, the total incident flux is $2\pi\int_0^{\frac{1}{2}\pi} N_s(\psi)\cos\psi\sin\psi\,d\psi$. Hence the albedo is given by

$$R = \int_0^{\frac{1}{2}\pi} N(\mu)\sin 2\mu\,d\mu \Big/ \int_0^{\frac{1}{2}\pi} N_s(\psi)\sin 2\psi\,d\psi\,. \tag{26}$$

TABLE I. Albedo of Sea to Sky Light

Sky \ Sea	*Smooth* ($\sigma = 0$)	*Rough* ($\sigma = 0.2$)
Clear	.100	.071 – .088
Uniform	.066	.050 – .055
Overcast	.052	.043 – .044

The albedo has been evaluated numerically for a smooth and rough sea surface for each of the three sky conditions shown in Fig. 6. In the case of the rough surface, the integration was carried out along both branches of the curve $\sigma = 0.2$ in Fig. 7; the correct values are

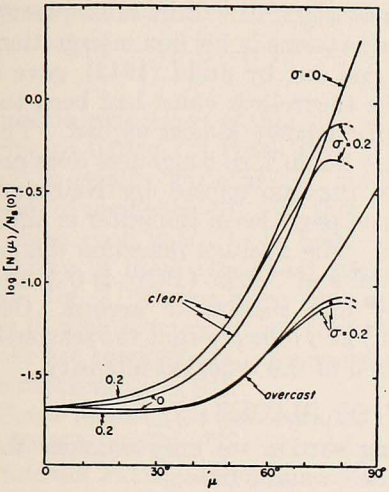

Figure 7. The radiance of the sea surface, $N(\mu)$, divided by the sky radiance at the zenith, $N_s(0°)$, as a function of the vertical angle μ. The curves are computed for a flat ($\sigma = 0$) and rough ($\sigma = 0.2$) surface for each of the three sky conditions illustrated in Fig. 6. The two branches for the curves marked $\sigma = 0.2$ again indicate the upper and lower limits inherent in equations (19) and (20).

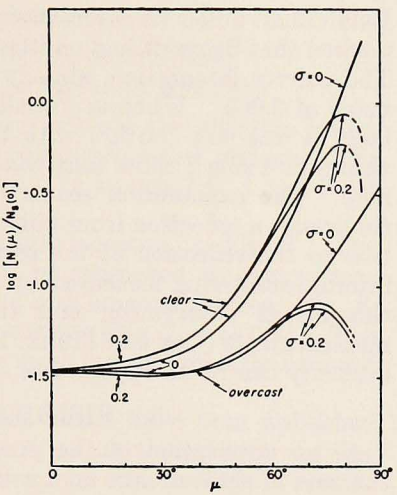

Figure 8. The radiance of a slick sea surface (see legend of Fig. 7).

believed to lie within the indicated limits. Compared to a flat sea, the albedo is reduced by about 20% in the presence of a Beaufort 4 wind, due largely to the hiding of effectively reflecting slopes and to subsequent darkening of the sea surface near the horizon.[7]

For the uniform sky, Schmidt (1915) had previously obtained a theoretical value of 0.17. Measurements by Neiburger (1948) and

[7] Note added in proof: Burt (1954) has calculated the albedo of the sea surface to direct sunlight and diffused light by methods similar to ours. However, there are two important differences. Burt made no allowance for multiple reflections but he allowed for shadowing by assuming the *same* distribution of slopes in the shadowed and unshadowed areas. For very low sun elevations he obtains 100% effective reflectivity regardless of surface roughness, whereas our approximation indicates a lowering of reflectivity which increases in magnitude with increasing roughness. Applied to the reflection of skylight, Burt's result implies that there would be no contrast at the horizon, while in fact the sea is darker than the sky, particularly on windy days. Fortunately the albedo to skylight is little effected by any of these assumptions. For $\sigma = 0.2$, Burt obtains $R = .058$ (clear sky), .048 (overcast), while our values are .050 — .055 (clear), .043 — .044 (overcast).

Burt (1953) under an overcast sky gave only 0.10. Burt subsequently noticed that Schmidt had omitted cosine terms in his flux intergration. The correct integration, already carried out by Judd (1942), gave a value of 0.066. Whereas initially the theoretical value had been too high, it was now too low with the discrepancy almost as bad. The values in Table I show that allowance for surface roughness does not help. The explanation seems to be the one offered by Neiburger (in press): a reflection from bubbles and particles in the water in addition to the reflection at the surface. The average reflection due to internal scattering measured by Powell and Clarke (1936) is 0.3, and this brings observation and theory into reasonable accord. Our measurements (Cox and Munk, 1954a) also indicate that the scattered intensity can be an appreciable fraction of the reflected intensity.

5. VISIBILITY OF SLICKS

As an application of the preceding section we may consider the contrast of slick streaks on a roughened water surface.

A slick is caused by the presence on the sea surface of a thin layer of organic matter. Natural slicks are often thin compared to the wave length of light, and the reflection coefficient of a slick surface is practically the same as that of an uncontaminated surface. The thin layer becomes visible because the rms slope is substantially smaller there than elsewhere. This reduction is accomplished, at least in part, by the viscous dissipation of wavelets against the quasi-inextensible surface film. The reduction in slope in a good sized slick may be achieved by a factor of 1.5 to 2 (Cox and Munk, 1954b).

A slick lying *within* the sun's glitter pattern has a larger luminosity near the glitter center and a smaller luminosity near the outer edges than the uncontaminated water surface. This has already been discussed (Cox and Munk, 1954b) and an example is shown in fig. 2 of that paper. The visibility of thin (natural) slicks *outside* the sun's glitter can be discussed with reference to Fig. 7. To an observer looking steeply downward (small μ), the slick (small σ) appears dark under a clear sky, light under an overcast sky. Near the horizon the slick is always light. The contrast required for the visibility of large slicks is of the order of 2% ($\sim$ 0.01 on the logarithmic scale in Fig. 7), and we may expect adequate contrast for visibility even when the winds are light. In searching for thin slicks one should concentrate on an area well toward the horizon in clear weather.

The situation is different in the case of freshly spread slicks of mineral oil. The presence of interference colors demonstrates a thickness larger than a wave length of light. Suppose the index of refraction is that of light oil, $n = 1.45$, as compared to 1.34 for water.

For normal incidence the reflectivities are

$$(n - 1)^2 (n + 1)^{-2} = 0.034 \text{ for air-oil interface,}$$
$$= 0.020 \text{ for air-water interface.}$$

Multiple reflections within the oil layer increase the effective reflectivity to 0.036, 1.8 times that of an uncontaminated surface. The ratio is smaller for glancing incidences. It equals 1.6, 1.3, 1.0 for angles of incidence 30°, 60°, 90°.

These coefficients have been taken into account in Fig. 8. The visibility of thick (artificial) slicks can be estimated by comparison with Fig. 7. Suppose we compare the oily smooth surface (Fig. 8, $\sigma = 0$) with the uncontaminated rough surface (Fig. 7, $\sigma = 0.2$). The slicks are brighter, and the contrast is most marked directly beneath the observer ($\mu = 0°$).

Some remarkable photographs of slick bands have been published by Ewing (1950). The surprising aspect is that these bands are due to *internal* waves. These are made visible by a curious chain of events: the orbital motion of the internal waves converges at the troughs and the oils resulting from biological activity are squeezed into a surface-active film under tension, as shown by Ewing. This film, by virtue of its resistance to stretching, imposes a horizontally quasi-rigid boundary against which short wavelets generated by local winds dissipate most of their energy. The resulting decrease in mean square slope affects the average reflectivity and also the segment of sky that is mirrored in the trough zones; both of these effects produce a brightness contrast between the slicks and the surrounding ruffled water. It would seem that it is virtually impossible to predict the devious means by which nature chooses to reveal herself to the astute observer!

REFERENCES

Burt, W. V.

1953. A note on the reflection of diffuse radiation by the sea surface. Trans. Amer. geophys. Un., *34:* 199–200.

1954. Albedo over wind-roughened water. J. Meterol., *2:* 283–290.

Cox, Charles and W. H. Munk

1954a. The measurement of the roughness of the sea surface from photographs of the sun's glitter. J. opt. Soc. Amer., *44:* 838–850.

1954b. Statistics of the sea surface derived from sun glitter. J. Mar. Res. *13:* 198–227.

Duntley, S. Q.

1950. The visibility of submerged objects: Part I, Optical effects of water waves. Visibility Laboratory, Mass. Inst. Techn. Report, Dec. 15, 1950, or U. S. Office of Naval Research Report No. N5 ori-07831.

Ewing, Gifford

1950. Slicks, surface films and internal waves. J. Mar. Res., *9*: 161–187.

JUDD, D. B.
1942. Fresnel reflection of diffusely incident light. J. Res., Nat. Bur. Stand., *29:* 329–332. Research Paper 1504.
MOON, PARRY AND D. E. SPENCER
1942. Illumination from a non-uniform sky. Ill. Eng., *37*; 707–726.
NEIBURGER, MORRIS
1948. The reflection of diffuse radiation by the sea surface. Trans. Amer. geophys. Un., *29:* 647–652.
1954. A note on the reflection of diffuse radiation by the sea surface. Trans. Amer. geophys. Un. (in press).
POWELL, W. M. AND G. L. CLARKE
1936. The reflection and absorption of daylight at the surface of the ocean. J. opt. Soc. Amer., *26:* 111–120.
RICHARDSON, R. A. AND E. O. HULBURT
1949. Sky brightness measurements near Bocaiuva, Brazil. J. geophys. Res., *54:* 215–227.
SCHMIDT, WILHELM
1915. Strahlung and Verdunstung an freien Wasserflächen; ein Beitrag zum Warmehaushalt des Weltmeers und zum Wasserhaushalt der Erde. Ann. Hydrogr., Berl., *43:* 111–124.
SCHOOLEY, A. H.
1954. A simple optical method for measuring the statistical distribution of water surface slopes. J. opt. Soc. Amer., *44:* 37–40.